DETERMINING THE COEFFICIENT OF CIRCULAR TEMPLATE FOR FAST SIMILARITY MEASUREMENT IN IMAGE REGISTRATION

Chul-Soo Ye (1)

[1] Far East Univ., 76-32 Daehakgil, Eumseong-gun, Chungbuk, 27601, Korea,
Email: csye@kdu.ac.kr

KEY WORDS: Image registration, Circular template, Mutual information.

ABSTRACT: Image registration is a very important process for change detection in remote sensing. To align two different images over a certain area, we first need to detect a feature point in a reference image using appropriate corner detects and then find the corresponding feature point in the other image by computing the similarity between the two feature points using a matching template. Though the circular template matching based on mutual information has shown good matching performance in image registration, it has a weakness of the long time in similarity computation. In this paper, we propose a method to design the coefficient of the circular template for fast similarity measurement. As the location, i.e., the coefficient of the circular template used for similarity computation, we select only the locations at a certain interval along the radial direction and the circumference of circular template. By combining this scheme with scale factors, we create various kinds of circular templates. The experimental results showed that the proposed method reduced the computation time significantly while maintaining the matching accuracy. In the case of the sampling scheme without scale factors, the representative results showed that the ratio of running time to the original circular template was in the range from 1.97% to 2.06%. The sampling scheme with scale factors showed that the ratio of running time to the original circular template was in the range from 1.82% to 2.21%.

1. INTRODUCTION

The technical advance in image sensors and platforms such as satellites and unmanned aerial vehicles provides us more opportunities to acquire the images for remote sensing in various conditions. The analysis based on multi-resolution and multi-temporal images requires the image registration between two or more images to align the images in one image coordinate system. The image registration has three steps: feature point detection, feature point matching and image transformation using the matched feature points. The feature point detection is one of basic issues in image processing.

As a feature point, the corner point is commonly used in remote sensing and image processing fields. Various corner detectors (Harris and Stephens, 1988; Shi and Tomasi, 1994; Carneiro and Jepson, 2002; Ye, 2014a) have been proposed including Harris corner detector, which is a popular corner detector and has been used widely for feature detection in image processing. The detected corners are used in feature point matching between images. The feature point matching is a process to find the corresponding point in the other image of the feature point. Scale Invariant Feature Transform (SIFT)-based descriptor is well known image descriptor for image registration (Lowe, 2004; Song *et al*., 2014; Gong *et al*., 2013; Sun *et al*., 2014). SIFT-based descriptor, however, is not suitable for detection of corners such as road junction, while it is suitable for blob-like features (Wu *et al*., 2012). Ye (2018) proposed a feature matching method using variable circular template, which has an advantage of rotation invariance property in image matching and also employs mutual information as similarity measure. The circular template matching based on mutual information using a large size of template needs a long processing time to compute similarity between images. In this paper, we propose a method to determine the coefficient of circular template for fast similarity measure.

2. METHODOLOGY

2.1 Circular Template

The template for similarity measurement has normally rectangular shape because of its easy implementation. The rectangular template has the drawback of variant property under the condition of image rotation. i.e., the rectangular template covers a little different area when an image is rotated or a template is rotated, compared to the condition that neither the image nor the template is rotated. In contrast, the circular template has rotation invariant property, which is an important property in finding corresponding points between images under rotation transformation. The coefficients of circular template can be easily transformed from image coordinates to polar coordinates using simple

formula as shown in Figure 1 (Ye, 2018). The location of each coefficient in the circular template is transformed to the element of two-dimensional array. The elements of each column represent the coefficients located along radial direction from the center of circular template.

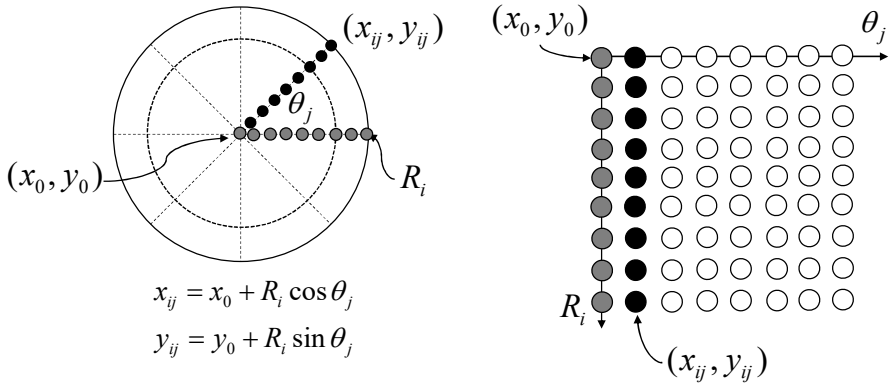

Figure 1. Coefficients of circular templates (left) transformation of coefficients of the circular template from image coordinates to polar coordinates (right) two-dimensional array for the coefficients of the circular template.

2.2 Similarity Measurement Using Mutual Information

To find the corresponding feature point of the reference image in the test image, we computer the similarity between the circular template centered at the feature point in the reference image and the moving circular template in the test image. We employ mutual information as similarity measure to compute the similarity between the two circular templates. The pixel located at the center of the moving circular template with maximum mutual information is accepted as the matched pixel of the feature point in the reference image. The mutual information *M* is computed using the following formula:

$$M = H(C_R) + H(C_T) - H(C_R, C_T) \tag{1}$$

where $H(C_R)$ and $H(C_T)$ represent the entropy of the circular template C_R in the reference and the circular template C_T in the test image, respectively. $H(C_R, C_T)$ represents the joint entropy of a pair of pixels from the circular template C_R and the circular template C_T. The entropy requires the computation of the histogram of each circular template, which results in lots of computation. For example, the computation of entropy needs to calculate a histogram of 256 levels for an 8-bit grey image. Moreover, the computation of joint entropy needs more calculation due to the joint distribution of 256 x 256 levels for each location of moving circular template. Another issue of computation time is the size of circular template. The size of circular template should be larger than 100 pixels to obtain stable matching result (Ye, 2014b).

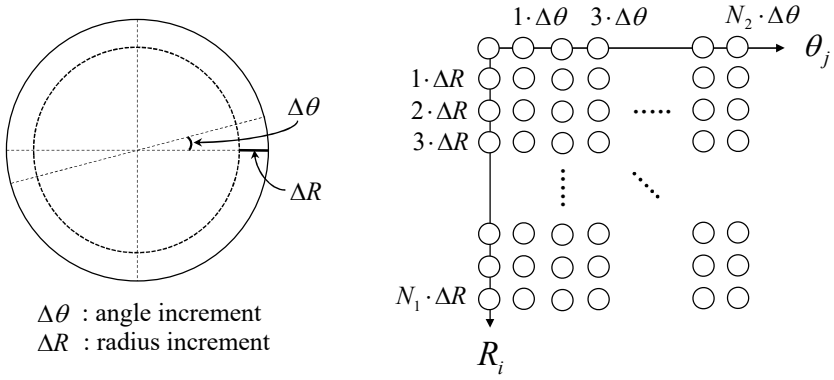

Figure 2. The relationship between the increments of angle and radius in circular template and two-dimensional array arrangement. If the angle and radius increments of the circular template are increased, then the numbers of angle and radius increments along circumference and radial direction decreases.

If the angle increment and the radius increment are given as $\Delta\theta$ and ΔR, respectively as shown in Figure 2, the two-dimensional array contains the total number N_T of elements, which is given as follows:

$$N_T = (N_1 + 1)\cdot(N_2 + 1) \tag{2}$$

where N_1 and N_2 are the total numbers of elements along radial direction and circumference of circular template,

respectively. If the angle increment is one degree ($\pi/180$), the radius increment is one pixel and the circular template has the radius of 300 pixels, then the total number N_T of elements in the two-dimensional array is given as follows:

$$N_T = (N_1 + 1) \cdot (N_2 + 1) = (300 + 1) \cdot (360 + 1) = 108{,}661 \quad (3)$$

This means that if all the elements of circular template are used for similarity measurement, then the computation time will increase greatly. To reduce the computation time, we need to choose selectively the elements of circular template for similarity measurement.

2.3 Selection of Circular Template Coefficient

The objective of selection of circular template coefficient is to fine the elements of circular template suitable for similarity measurement satisfying two conditions: decrease of computation time and low-level matching error. The adjacent elements of circular template covers adjacent or close pixels in the image. The adjacent or close pixels may work as redundant information in the computation of mutual information. Therefore, the selection of circular template coefficient can be classified into five types according to the sampling method as shown in Figure 3.
Type A selects all the elements of circular template. This type may produce relatively good matching performance while the computation time will increase greatly compared to the other types. Type B selects the elements located at an interval along the circumference of circular template. The interval along the circumference is determined by adjusting the angle increment $\Delta\theta$. For example, if the angle increment $\Delta\theta$ is $\pi/4$, then the number N_2 of the along the circumference of circular template becomes eight. Type C selects the elements located at an interval along the radial direction of circular template. The interval along the radial direction is determined by adjusting the radius increment ΔR . For example, if the radius increment ΔR is 3 and the circular template has the radius of 300 pixels, then the number N_1 of the along the radial direction of circular template becomes 100. Type D selects the elements located at intervals both along the circumference and the radial direction, respectively. This type is a kind of mixed type of Type B and Type C. Type E selects the elements located at a distance from the center of circular temple.

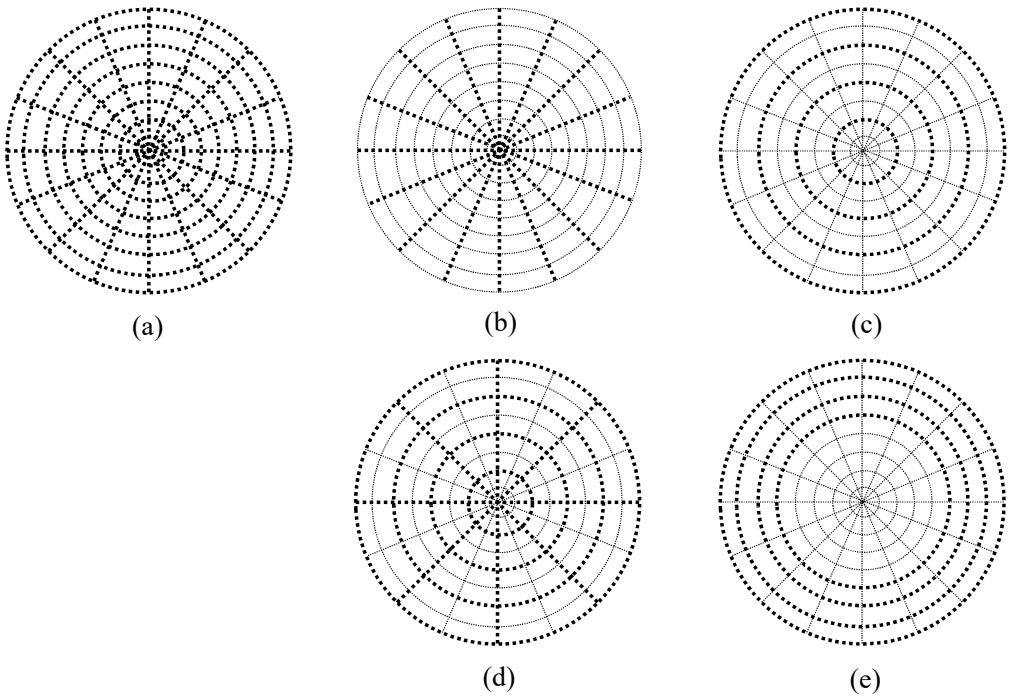

Figure 3. Types of circular template according to the sampling method. The thick dotted lines represent the elements to be selected for similarity measurement (a) Type A: all elements of circular template are used. (b) Type B: the elements located at an interval along the circumference are used (c) Type C: the elements located at an interval along the radial direction are used (d) Type D: the elements located at intervals both along the circumference and the radial direction, respectively, are used (e) Type E: the elements located at a distance from the center of circular temple are used.

Type E can be also combined with Type B and Type C as shown in Figure 4. Figure 4 (a) and (b) shows the circular

template Type E and its two-dimensional array arrangement, respectively. Figure 4 (c) and (d) shows the two-dimensional array arrangements of Type E combined with Type B and Type C, respectively. Therefore we can define the various types of circular templates as shown in Table 1. Type E-B and Type E-C represent the Type E combined with Type B and Type C, respectively. Type E-BC represents Type E combined with both Type B and Type C.

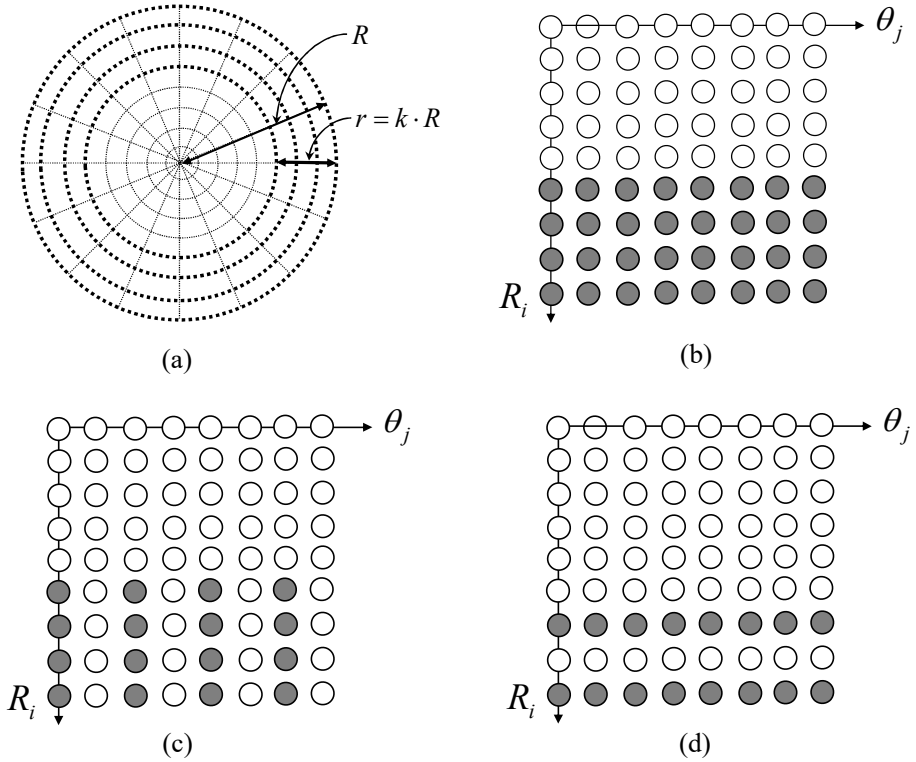

Figure 4. Combination of Type E with Type B and Type C (a) circular template of Type E (k is a scale factor with the range of 0.2 to 0.9) (b) two-dimensional array arrangement of Type E (c) two-dimensional array arrangement of Type E combined with Type B (d) two-dimensional array arrangement of Type E combined with Type C.

Table 1. Various types of circular templates

Circular Template Type	Radius increment ΔR	Angle increment $\Delta\theta$ (degree)	Scale factor k
Type A	{1}	{1}	{1}
Type B	{1}	{2,3, …,39}	{1}
Type C	{2,3,. .,29}	{1}	{1}
Type D	{2,3,. .,14}	{2,3, …,39}	{1}
Type E	{1}	{1}	{0.1,0.2, …,0.9}
Type E-B	{1}	{2,3, …,39}	{0.2, 0.3, …,0.9}
Type E-C	{2,3,. .,14}	{1}	{0.2, 0.3, …,0.9}
Type E-BC	{2,3,. .,14}	{2,3, …,39}	{0.2, 0.3, …,0.9}

3. EXPERIMENTAL RESULS

3.1 Study Area and Datasets

As the experimental images, we used Kompsat-3A and Kompsat-3 images of Niamey, which were acquired on November 29, 2015 and January 21, 2013, respectively as shown in Figure 5. We selected a corner point from Kompsat-3A and its corresponding corner point from Kompsat-3 images, respectively (Figure 5 (c) and (d)). The two images have the differences of spatial resolution and rotation angles. We assume that the information about the difference of scale and rotation between two images is given in advance and evaluate the time requiring for feature matching and the performance of matching accuracy. The initial circular template used for Type A has the radius R of 300 pixels. All the types of circular templates in Table 1 were tested using each parameter of radius increment,

angle increment and scale factor. For example, the radius increment and the angle increment are given as $\Delta R = 1$ and $\Delta\theta = \{ 2^\circ, 3^\circ, ..., 39^\circ \}$ in the circular template Type B. In the circular template Type E-BC, for each scale factor *k*, we create various circular templates with the radius increment in the range of 2 to 14, and with the angle increment in the range of 2° to 39°. The experiments was carried out using a laptop with Intel core i7-8850H processor (2.60 GHz) and 64GB DDR4 memory.

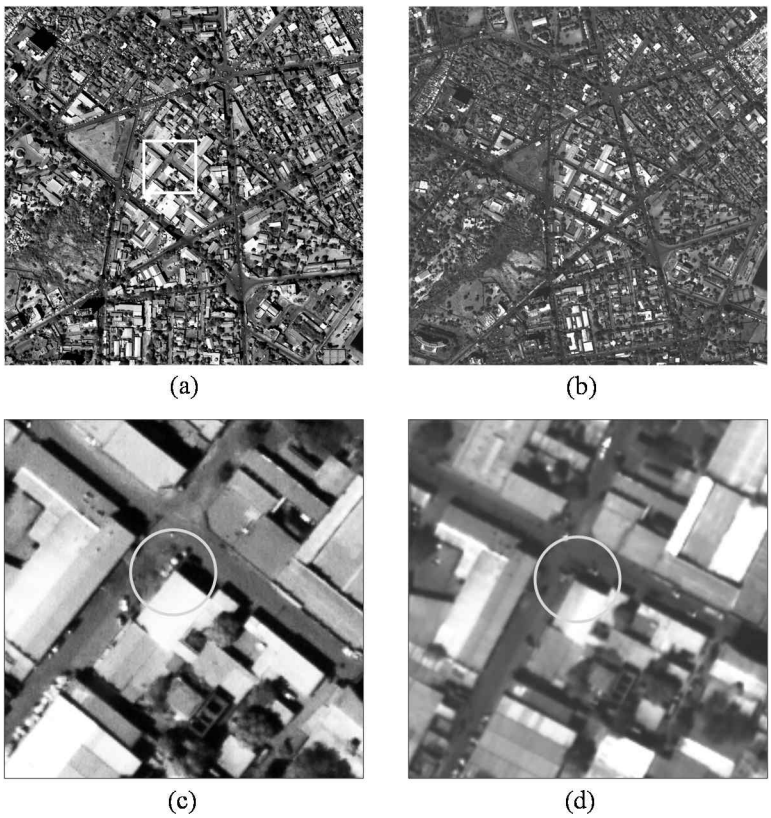

Figure 5.Test images of Niamey and feature points (a) Kompsat-3A (b) Kompsat-3 (c) a feature point (the center point of the white circle) in the enlarged Komspat-3A image of the white square area in Figure 5 (a) (d) the corresponding feature point in the enlarged Komspat-3 image.

3.2 Matching Results

Type A: The matching error of Type A circular template was zero and the running time for matching was 473.60 seconds. The matching error is the mean value of row and column matching errors between the matched point and the reference point.

Type B: The feature matching was carried out using the radius increment $\Delta R = 1$ for each angle increment $\Delta\theta = \{ 2^\circ, 3^\circ, ..., 39^\circ \}$. Figure 6 shows the matching error and the running time according to the change of angle increment. The matching errors are maintained below one pixel until the angle increment of 23 and then show a large variation. When the angle increment is 2°, the running time is 238.01 seconds, which is 50.3% of the running time of Type A. The running time keeps decreasing as the angle increment increases. The performance of running time shows remarkable increase when the angle increment goes up to 23° where the running time reaches 21.27 seconds, which is 4.5% of the running time of Type A.

Type C: For each radial increment $\Delta R = \{2,3,...,29\}$ and the angle increment $\Delta\theta$ of 2°, the matching errors are maintained below two pixels until the radius increment of 15 and then show a large variation. The tendency of the change of running time according to the radius increment was similar to that of Type B. The running time at the radius increment of 15 reaches 34.28 seconds, which is 7.24% of the running time of Type A and longer than that of Type B.

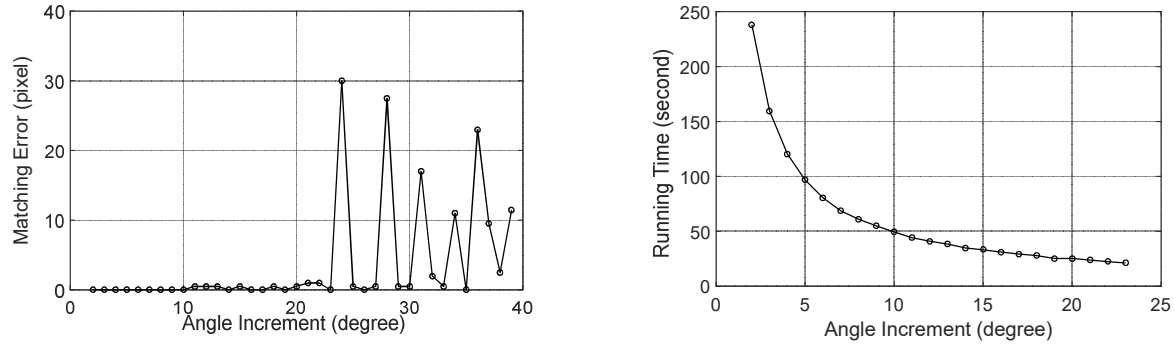

(a) (b)

Figure 6. Results of feature matching using the Type B circular template (a) matching error (b) running time for feature matching.

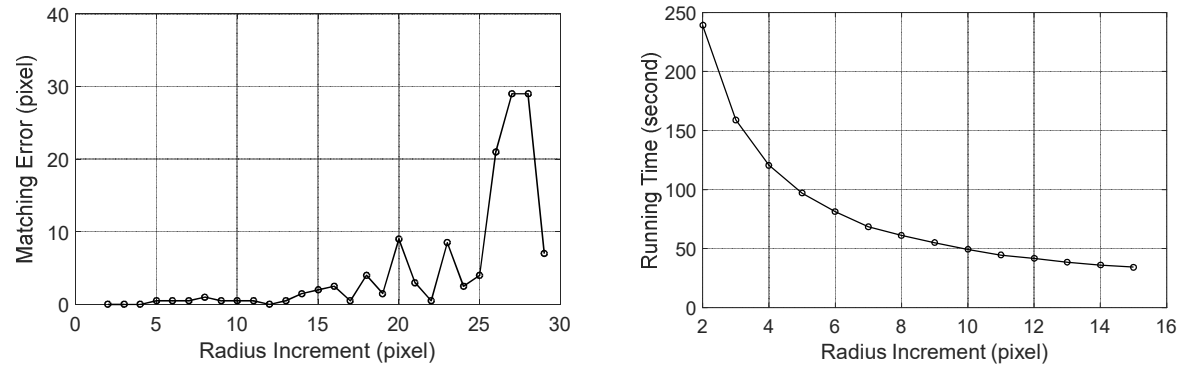

(a) (b)

Figure 7. Results of feature matching using the Type C circular template (a) matching error (b) running time for feature matching.

Type D: For each combination of the angle increment $\Delta\theta = \{2^\circ, 3^\circ, ..., 39^\circ\}$ and the radial increment $\Delta R = \{2,3,...,14\}$, we computed the matching errors. Figure 8 shows the matching results for each combination of the two increments. The combination of the two increments belonging to the flat area with low matching errors in Figure 8 (a) shows good matching performance, while the running time of combination of the two increments belonging to the flat area is longer than the non-flat area in Figure 8 (b). Table 2 shows the representative combination of radius and angle increments in terms of the running time under the condition that the matching error is less than one pixel. The minimum running time of 9.34 seconds is corresponding to 1.97% of the running time of Type A. The multiplication $\Delta R \cdot \Delta\theta$ of radius increment and angle increment represents a small unit area defined by the radius increment and the angle increment in the two-dimensional array. The value of $\Delta R \cdot \Delta\theta$ in the four combination cases is 56 or 60 and this means that if the radius and angle increments are in the ranges of 4 to 8 and of 7 to 15, respectively, and also the multiplication $\Delta R \cdot \Delta\theta$ is in the range of 56 to 60, then this combination may produce a good performance in terms of the matching error and the running time.

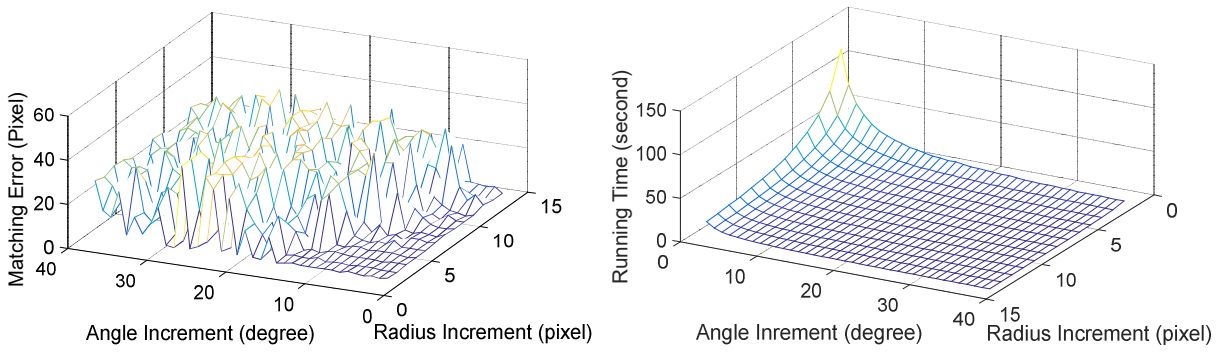

(a) (b)

Figure 8. Results of feature matching using the Type D circular template for each combination of the radial increment $\Delta R = \{2,3,...,14\}$ and the angle increment $\Delta\theta = \{2^\circ, 3^\circ, ..., 39^\circ\}$.

Table 2. Representative combination of radius and angle increments in terms of the running time

Radius increment ΔR	Angle increment $\Delta\theta$	$\Delta R \cdot \Delta\theta$	Matching error (pixel)	Running time (second)	Ratio of running time to Type A (%)
4	15	60	0	9.34	1.97
5	12	60	1	9.36	1.98
7	8	56	1	9.77	2.06
8	7	56	1	9.69	2.05

Type E: Type E is similar to Type A except that the matching area of circular template is limited by a scale factor *k*. If the scale factor *k* is 0.1, then the inner boundary of circular template becomes (1-0.1)*R*=0.9*R*, i.e., the area of circular template between 0.9*R* and *R* is used for matching. As the scale factor *k* becomes large, the area of circular template used for matching becomes large and the matching error becomes small as shown in Figure 9 (a), while the running time increases as the scale factor becomes large as shown in Figure 9 (b). This means that if we want to obtain a small matching error, then the scale factor should be large enough to include sufficiently the area of circular template. For example, the scale factors k = 0.5, 0.6 and 0.7 show good matching errors less than 0.5 pixels and also take much less running times than Type A.

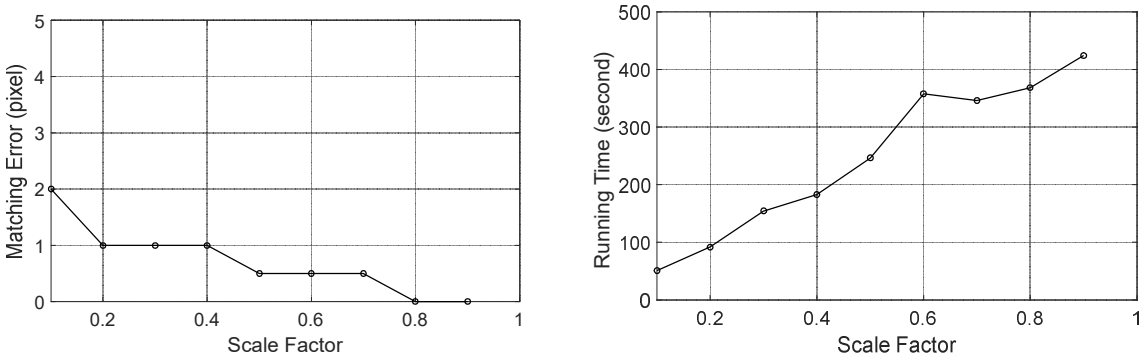

(a) (b)

Figure 9. Results of feature matching using the Type E circular template (a) matching error (b) running time for feature matching.

Type E-B: Type E-B is similar to Type B except that the matching area of circular template is limited by a scale factor *k*. The tendency of matching results of Type E-B is similar to that of Type B except that the running time becomes smaller for a fixed angle increment. Figure 10 shows the results of Type E-B with the scale factor *k*=0.5 and the running time is about half of that of Type B. For example, for the angle increment $\Delta\theta$ =5, the running time of Type E-B is 51.35 seconds, while that of Type B is 96.92 seconds.

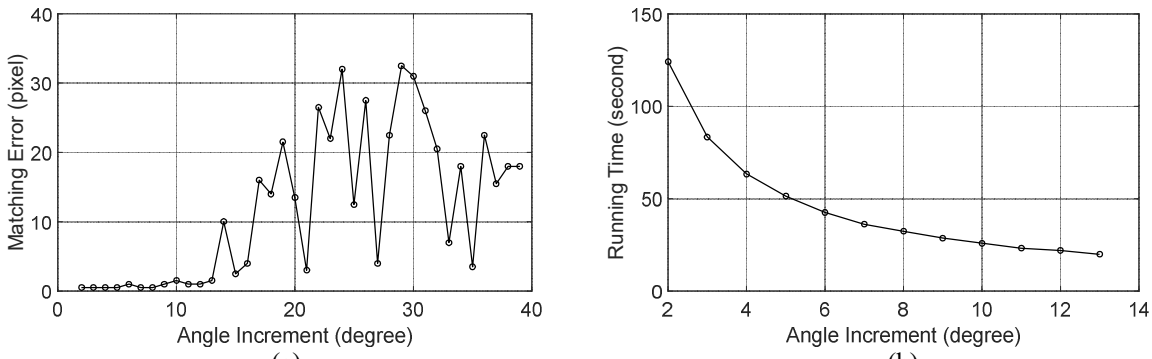

(a) (b)

Figure 10. Results of feature matching using the Type E-B circular template (scale factor *k*=0.5) (a) matching error (b) running time for feature matching.

Type E-C: Type E-C is similar to Type C except that the matching area of circular template is limited by a scale factor *k*. The tendency of matching results of Type E-C is similar to that of Type B except that the running time becomes smaller for a fixed radius increment. Figure 11 shows the results of Type E-C with the scale factor *k*=0.5 and the running time is about half of that of Type C. For example, for the radius increment $\Delta R = 5$, the running time of Type E-C is 51.51 seconds, while that of Type C is 97.07 seconds.

Type E-BC: Type E-BC is similar to Type D except that the matching area of circular template is limited by a scale factor *k*. Figure 12 shows the comparison of running time depending on the four scale factors. For each scale factor and radius increment, we find the minimum running time in the range of angle increments satisfying the constraint that the matching error is less than two pixels. A relatively short amount of running time has been obtained in the range between 3 and 6 of the radius increment for the four scale factors. Table 3 shows the representative combination of radius and angle increments in terms of the running time under the condition that the matching error is less than 1.5 pixels. The value of $\Delta R \cdot \Delta\theta$ in the four combination cases is 40 or 48, which is a little smaller than that of Type 4. The ratio of running time to Type A is in the range from 1.82% to 2.21%. The running time of 8.60 seconds for the scale factor k=0.6, is the minimum value in the all experimental tests using the various types of circular templates.

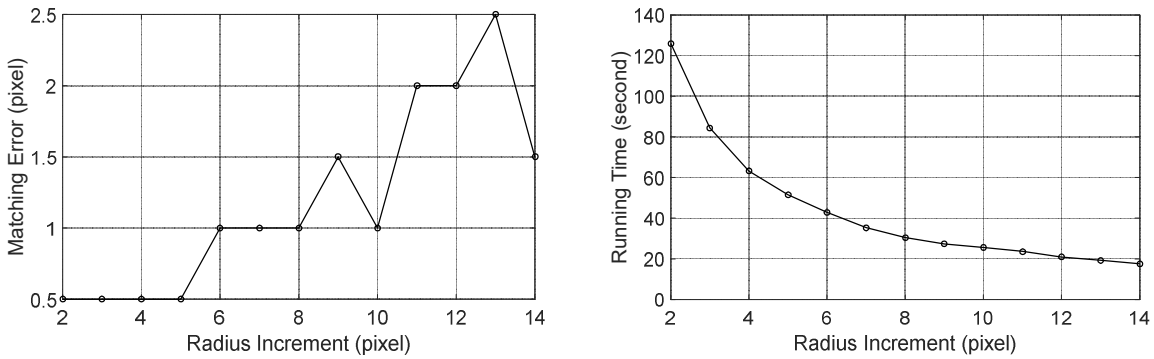

(a) (b)

Figure 11. Results of feature matching using the Type E-C circular template (scale factor k=0.5) (a) matching error (b) running time for feature matching.

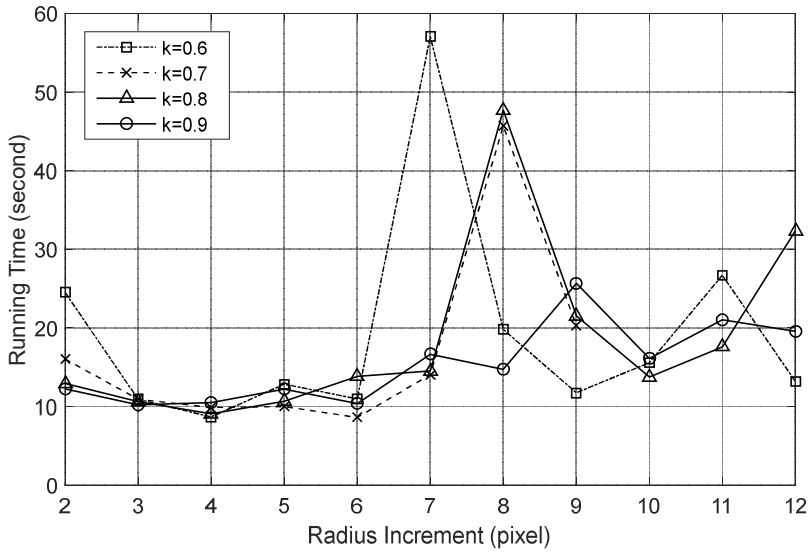

Figure 12. Results of feature matching using the Type E-BC circular template (scale factor k=0.5) (a) matching error (b) running time for feature matching.

Table 3. Representative combination of radius increment and angle increment in terms of the running time

Scale factor k	Radius increment ΔR	Angle increment $\Delta\theta$	$\Delta R \cdot \Delta\theta$	Matching error (pixel)	Running time (second)	Ratio of running time to Type A (%)
0.6	4	10	40	1.5	8.67	1.83
0.7	6	8	48	1	8.60	1.82
0.8	4	12	48	1	9.06	1.91
0.9	4	12	48	1	10.48	2.21

4. CONCLUSIONS

In this paper, a method to select coefficients of circular template was proposed. By sampling the locations at a certain interval along the radial direction and the circumference of circular template, respectively, we can create two types of circular templates (Type B and Type C). When the sampling scheme is applied simultaneously to the radial direction and the circumference of circular template, then another type of circular templates is created (Type D). If this scheme is combined with a scale factor, we can create various kinds of circular templates (Type E ~ Type E-BC). By using Type B and Type C circular templates, the running time was reduced to 4.5% and 7.24% of the running time of the original circular template (Type A) while maintaining the matching accuracy. The combination of radius and angle increments in the Type D produced more improvement results than Type B and Type C in terms of the running time. The representative results of Type D showed that the ratio of running time to Type A was in the range from 1.97% to 2.06%. The circular templates combined with a scale factor showed that the running time becomes smaller for a fixed radius increment. The result of representative combination of radius increment and angle increment in Type E-BC showed that the ratio of running time to Type A was in the range from 1.82% to 2.21%. We obtained a relatively short amount of running time in the range between 3 and 6 of the radius increment for the four scale factors.

ACKNOWLEDGMENT

This research was supported by Basic Science Research Program through the National Research Foundation of Korea (NRF) funded by the Ministry of Education (No. 2018R1D1A1B07048266).

REFERENCES

Carneiro, G. and A. D. Jepson, 2002. Phase-based local features, Proc. of the 7th European Conference on Computer Vision, Copenhagen, Denmark, May 28-31, vol. 1, pp. 282-296.

Gong, M., S. Zhao, L. Jiao, D. Tian, and S. Wang, 2014. A novel coarse-to-fine scheme for automatic image registration based on SIFT and mutual information, IEEE Transactions on Geoscience and Remote Sensing, 52(7): 4328-4338.

Harris, C. and M. Stephens, 1988. A combined corner and edge detector, Proc. of the 4th Alvey Vision Conference, Manchester, UK, Aug. 31-Sep. 2, pp. 147-151.

Lowe, D. G., 2004. Distinctive image features from scale-Invariant keypoints, International Journal of Computer Vision, 60(2): 91-110.

Shi, J. and C. Tomasi, 1994. Good features to track, Proc. of IEEE conference on Computer Vision and Pattern Recognition, Seattle, USA, Jun. 21-23, pp. 593-600.

Song, Z., S. Zhou, and J. Guan, 2014. A novel image registration algorithm for remote sensing under affine transformation, IEEE Transactions on Geoscience and Remote Sensing, 52(8): 48954912.

Sun, Y., L. Zhao, S. Huang, L. Yan, and G. Dissanayake, 2014. L2-SIFT: SIFT feature extraction and matching for large images in large-scale aerial photogrammetry, ISPRS Journal of Photogrammetry and Remote Sensing, 91: 1-16.

Wu, B., Y . Zhang, and Q. Zhu, 2012. Integrated point and edge matching on poor textural images constrained by self-adaptive triangulations, ISPRS Journal of Photogrammetry and Remote Sensing, 68: 40-55.

Ye, C.H., 2014a. Feature detection using geometric mean of eigenvalues of gradient matrix, Korean Journal of Remote Sensing, 30(6): 769-776.

Ye, C.S., 2014b. Mutual information-based circular template matching for image registration, Korean Journal of Remote Sensing, 30(5): 547-557.

Ye, C.H., 2018. Feature matching using variable circular template for multi-resolution image registration, Korean Journal of Remote Sensing, 34(6-3): 1351-1367.